

1 **GEE-PICX: Generating cloud-free Sentinel-2 and**
2 **Landsat image composites and spectral indices**
3 **for custom areas and time frames - a Google**
4 **Earth Engine web application**

5

6 **LUISA PFLUMM^{1,2}, HYEONMIN KANG^{1,2,3}, ANDREAS WILTING¹, JÜRGEN NIEDBALLA^{1*}**

7

8 *¹ Leibniz Institute for Zoo and Wildlife Research, Alfred-Kowalke-Str. 17, 10315 Berlin, Germany*

9 *² University Würzburg, Sanderring 2, 97070 Würzburg*

10 *³ Nadar GmbH, Kasseler Str. 42, 04155 Leipzig, Germany*

11

12 * Corresponding author: niedballa@izw-berlin.de

13

14

15

16

17

This manuscript is a non-peer-reviewed preprint submitted to EarthArXiv.

18 Abstract

19

20 Earth observation satellites are collecting vast amounts of free and openly accessible
21 data with immense potential to support environmental, economic, and social fields. As the
22 availability of remotely sensed data increases, so do the methods for accessing and
23 processing it. Many solutions exist for creating cloud-free image composites from often
24 cloudy satellite data, but these typically require coding skills or in-depth training in remote-
25 sensing techniques. This technical barrier prevents many researchers and practitioners
26 from utilising available satellite data. The few user-friendly solutions that exist often have
27 limitations in terms of data export size and quality assessment capabilities. We developed
28 *GEE-PICX*, a web application with an intuitive graphical user interface on the cloud
29 computing platform Google Earth Engine. This tool addresses the aforementioned
30 challenges by creating cloud-free, analysis-ready image composites for user-defined
31 areas and time periods. It utilises Sentinel-2 and Landsat 5, 7, 8, and 9 images and offers
32 global coverage. Users can aggregate image composites annually or seasonally, with
33 data availability starting from 1984 (the launch of Landsat 5). The workflow automatically
34 filters all available satellite data according to user input, removing clouds, cloud shadows,
35 and snow. It provides spectral band information, calculates various thematic spectral
36 indices (including vegetation, burn, built-up area, bare soil, snow, moisture, and water
37 indices), and includes a quality assessment band indicating the number of valid scenes
38 per pixel. *GEE-PICX* offers a customizable tool for creating custom data products from
39 freely accessible satellite data, catering to researchers with limited remote sensing
40 experience. It provides extensive temporal and global spatial coverage, with server-side
41 processing eliminating hardware constraints. The tool facilitates easy export of time series
42 as ready-to-use rasters with numerous spectral indices, supporting environmental
43 programmes and biodiversity research across various disciplines.

44

45 Introduction

46 Understanding environmental changes such as deforestation, desertification,
47 urbanisation, or the expansion of croplands over time is of utmost importance for
48 quantifying and managing the anthropogenic impacts on earth and to support sustainable
49 development and environmental protection (Chaves et al., 2020; Mallinis & Georgiadis,
50 2019; Weng et al., 2008). Satellite remote sensing is a widely used method for monitoring
51 such environmental changes due to the multitude of available sensors and platforms
52 providing continuous data of the earth's surface (Cord et al., 2017). Remote sensing data
53 is often freely available (e.g. Landsat since the 1980s), enabling scientists to monitor and
54 quantify short- and long term environmental changes.

55 Optical remote sensing imagery provides (multi-)spectral information, yet the presence of
56 clouds, cloud shadows, and highly reflective surfaces such as snow can adversely affect
57 sensor measurements, posing challenges in acquiring unbiased and gap-free information
58 (Zhu et al., 2015). Opaque clouds cover approximately 31% of the Earth's surface on
59 average at any time (Guzman et al., 2017), necessitating automatic detection and
60 accurate removal from remote sensing data prior to analysis to prevent data errors at the
61 respective positions. Cloud removal causes gaps in satellite images which can complicate
62 analysis. This can be overcome by merging multiple images from different time points to
63 create cloud-free and gap-free image products. These composite products can then be
64 used for land cover classifications (Verhoeven & Dedoussi, 2022), land monitoring
65 applications (Carrasco et al., 2019; Parmes et al., 2017), time series analyses
66 (Lasaponara et al., 2022; Yin et al., 2020) or spatial modelling (Guharajan et al., 2021).

67 After cloud-correction, multi-spectral information can either be used directly (Zhu et al.,
68 2018) or via derived spectral indices, which are combinations of the spectral reflectance
69 from two or more wavelengths (Chaves et al., 2020; Rudd et al. 2021). Spectral indices
70 are often more suitable for specific analyses than raw spectral information due to more
71 clearly defined and interpretable properties (Rudd et al., 2021). The most popular spectral
72 indices are vegetation indices, but other indices e.g. for burned areas, man-made (built-

73 up) features, water or ice are available, too (Chaves et al., 2020; Montero et al., 2023;
74 Petropulos & Kalaitzidis, 2011).

75 The increasing availability of remote sensing data is accompanied by advancements in
76 software for managing large data sets and processing chains. In the geospatial
77 community, Google Earth Engine (GEE), a cloud computing platform powered by Google
78 Cloud infrastructure, has gained popularity for generating analysis-ready image products
79 for various applications across different spatial and temporal scales (Wu 2020;
80 Lasaponara et al., 2022; Piao et al., 2019; Yang et al., 2021). In recent years, developers
81 have created various tools and applications designed to streamline access and pre-
82 processing of satellite imagery, for example *ClimateEngine* (Huntington et al., 2017),
83 *Awesome Spectral Indices (ASI)* (Montero et al., 2023), *geemap* (Wu, 2020), *rgee* (Aybar
84 et al., 2020). Furthermore, platforms like *SentinelHub* (Sinergise, 2023a) or *EarthExplorer*
85 (United States Geological Survey, 2023) provide user-friendly access to large databases
86 of remote sensing data. While some of these tools require programming skills (*ASI*,
87 *geemap*, *rgee*), others offer more user-friendly interfaces, but have limitations such as
88 restricted downloads for larger areas (*ClimateEngine*, *SentinelHub*) or they do not provide
89 options for image aggregation or further data processing like spectral index calculation
90 (*EarthExplorer*). Thus, we developed *GEE-PICX*, a Google Earth Engine web application
91 providing advanced satellite data products for non-expert, which addresses these
92 limitations by offering cloud-masking, data aggregation, and spectral index calculation,
93 similar to *ClimateEngine* or *SentinelHub*. It also provides a novel quality assessment
94 band, specifying valid scenes per pixel in image aggregates. *GEE-PICX* allows for
95 significantly larger data downloads compared to other platforms, though visualisation of
96 large areas within the web application may be more limited than for smaller areas. Unlike
97 specialised tools for specific applications such as land-cover classification (REMAP,
98 Murray et al., 2018), or crop-climate-suitability mapping (Peter et al., 2020), *GEE-PICX*
99 focuses on providing flexible access to satellite data with optional spectral index and data
100 quality information. This approach ensures broad applicability across various research
101 domains and analysis types. For an overview and comparison of available applications,
102 see Supporting Information S1.

103 *GEE-PICX* generates, visualises and exports cloud-free, analysis-ready composites of
104 satellite images for user-defined areas and time steps, with global data coverage. We
105 followed five design principles in developing *GEE-PICX*:

- 106 **1. Flexibility of user input.** Users can select the satellite platform (Landsat or
107 Sentinel-2), study area boundaries, time range, maximum cloud cover (for single
108 images), aggregation mode, and image bands. Relevant scenes are automatically
109 selected from the data catalogue according to user input. Moreover, the modular
110 design allows users to easily add custom indices.
- 111 **2. Ease of use.** The application features a self-explanatory graphical user interface.
112 It only requires a Google account, web browser, and internet connection, with no
113 additional hardware or software requirements due to server-side processing.
- 114 **3. Export of large data sets.** Export size is limited only by Google drive storage
115 capacity.
- 116 **4. Generation of analysis-ready data.** Produces cloud-free image composites with
117 spectral bands, spectral indices, and a quality assessment band (valid scenes per
118 pixel). Export image resolution and coordinate reference system are customizable.
- 119 **5. Data visualisation.** Data sets can be visualised in the browser prior to export.

120 This paper presents *GEE-PICX*, a web-based application designed to simplify access to
121 satellite imagery analysis. Our objectives are to describe the technical workflow and
122 features of *GEE-PICX*, highlighting how it addresses common challenges in satellite data
123 processing, and demonstrate the tool's versatility through two diverse use cases in
124 ecological research. We then present two examples that illustrate the application of *GEE-*
125 *PICX* in different ecological contexts and discuss the potential impact of *GEE-PICX* on
126 broadening the use of remote sensing data across various disciplines.

127

128 Workflow description

129 Overview

130 Users can access the web application via the provided application link (see Data
131 availability). The script is written in JavaScript and commented to facilitate orientation. No
132 manual code adjustments are necessary. With the application running, users can define
133 parameters according to their requirements in the application interface next to the map.
134 The application then internally processes user inputs, executing functions for satellite
135 image (pre-)processing, visualisation, and export preparation. Data visualisations are
136 available directly in the application. The products can be exported at user-defined spatial
137 resolutions and coordinate systems and are ready to use for subsequent analyses.

138 User input

139 Below we provide a detailed overview of the choices users can make for creating
140 customised data exports. For advanced information on data processing see Supporting
141 Information S2.

142 **Satellite data:** The application can provide image composites based on either the
143 Landsat or the Sentinel-2 mission. Both Landsat and Sentinel-2 data sets consist of
144 atmospherically and topographically corrected Level-2A products that show surface
145 reflectance values with atmospheric correction applied. The data set choice can be based
146 on either the required spatial resolution or length of the time series. The earliest Level-2A
147 products from Landsat date back to 1984 (at 30m resolution), whereas Sentinel-2 Level-
148 2A products have been available since 2017 (at 10m resolution in the visible and NIR
149 spectrum). The availability of Landsat data from the late 1980s and early 1990s is much
150 lower than in recent years, when more Landsat missions are simultaneously acquiring
151 imagery at a higher temporal frequency. When selecting Landsat missions for analysis it
152 is important to consider the potential impact of the Landsat 7 scan line corrector (SLC)
153 failure. The SLC, which normally ensures continuous image capture, failed in 2003. This
154 failure resulted in data gaps affecting about 22% of each scene. While the overall image

155 quality remains intact, these gaps can limit the usability of Landsat 7 images for
156 applications requiring seamless coverage (United States Geological Survey, 2022).
157 However, researchers developed gap-filling techniques to mitigate this issue (Storey et
158 al., 2005). In GEE-PICX, when selecting Landsat as the platform, users have the option
159 to include imagery from all Landsat missions (5, 7, 8, 9) to create image composites, or
160 they can choose to include only Landsat-8 and 9 data, which avoids including erroneous
161 Landsat-7 images. However, Landsat-8 data are only available from 2013 and Landsat-
162 9 data from 2022. For more specific information on the satellite missions see Supporting
163 Information S3.

164 **Area of interest:** The boundary of the study area can be defined either by uploading a
165 shapefile as an Earth Engine asset (Google Earth Engine, 2021), or by manually drawing
166 a polygon on the Google Earth Engine map. Data coverage is global.

167 **Time period:** The time frame can be specified by year- and month range. By default,
168 scenes are aggregated for one year (months 1 - 12). Users can create seasonal image
169 aggregates by narrowing the selection to specific consecutive months (also crossing the
170 year boundary). Users can request export of imagery from multiple years at once.

171 **Cloud cover filter:** Optical satellite images may exhibit partial or complete cloud
172 coverage. The pixel-level cloud masks included in scenes cannot perfectly detect and
173 filter out all clouds and cloud shadows (Sanchez et al., 2020). Therefore, the cloud cover
174 percentage per scene is utilised to enhance the quality of image composites by removing
175 scenes exceeding a cloud cover threshold. By default, images with cloud cover exceeding
176 65% are excluded prior to aggregation. Opting for a 100% threshold includes all images
177 captured within the specified study area and time frame. Cloud masking leads to data
178 gaps in all images affected by cloud cover. If all scenes have data gaps at the same
179 pixels, the image composite will also have data gaps at this location.

180 **Image bands:** Users can select single or multiple spectral bands, as well as spectral
181 indices and a valid pixel band, by activating the corresponding checkboxes. Spectral
182 bands convey surface reflectance data and are correlated with chlorophyll and other
183 pigments, vegetation structure and water content (Petropulos & Kalaitzidis, 2012). Key

184 correlations include Green, Red, and Red-edge bands with chlorophyll and pigments, NIR
185 bands with leaf structure, and SWIR with vegetation structure and water content (Chaves
186 et al., 2020; Fernández-Manso et al., 2016). Spectral indices result from mathematical
187 combinations of the spectral bands (see Supporting Information S4 for details on all
188 available indices). The valid pixel band is a quality assessment layer specifying the
189 number of valid scene values that are aggregated at each pixel.

190 **Aggregation mode:** The aggregation mode determines which summary statistic is
191 applied to the pixel values of all selected images. Available choices are mean, median
192 and standard deviation.

193 **Coordinate system:** The application offers the choice to export rasters in UTM and WGS
194 84 (EPSG 4326) formats. If UTM is selected, the application automatically identifies the
195 appropriate zone. If the study area spans multiple UTM zones, images can only be
196 exported in WGS 84.

197 **Spatial pixel resolution:** The application provides the options to export images at four
198 different spatial resolutions ranging from 10 to 100 metres. Opting for high resolutions in
199 extensive study areas could yield products exceeding several gigabytes, potentially
200 posing challenges for subsequent analyses. Users should choose a resolution that
201 matches their research or monitoring objectives.

202 Image export

203 After initiating the export in the application user interface, users can inspect and execute
204 the actual image export(s) within the upper-right window via the *Console* and *Tasks* tabs
205 (see Data availability). Two image collections will be automatically added to the *Console*.
206 The first contains all individual satellite images after filtering, the second contains the
207 image aggregates available for export. Each annual / seasonal image that appears in the
208 *Tasks* manager needs to be exported individually. When clicking "Run", a pop-up window
209 will appear in which the user can optionally modify export names, coordinate reference
210 system, scale, export destination and file format.

211 The easiest way to save the files on a local computer is to export them to a Google drive
212 folder which is connected to the users' Google account, and then download the data from
213 there. Multiple image exports run in parallel and depending on study area size each export
214 can take from minutes to hours (or even days for study regions measuring hundreds of
215 thousands of square kilometres). When exporting large data sets, Google Earth Engine
216 splits each image into smaller tiles. After downloading them from Google Drive, they can
217 either be merged to a large contiguous mosaic, or be used as a virtual raster.

218 Except for the "valid-pixel" band, all band values of the export images are multiplied by
219 10,000. This allows the raster values to be stored as integer values (signed 16-bit) instead
220 of floating point values, thus reducing the file size of exports.

221 Google Earth Engine assigns a value of zero to data gaps in image composites during
222 export to Google Drive, potentially biasing subsequent analyses. We provide an R script
223 for converting zero values back to NA with the help of the valid pixel layer prior to further
224 analyses (see Data availability).

225 Data visualisation

226 Users can visualise their export data on the map by selecting either a spectral index or
227 various band combinations. Band combinations can highlight certain features (e.g.,
228 vegetation types, water bodies, and urban areas) due to correlations between measurable
229 biophysical properties on the Earth's surface and remotely sensed surface reflectance
230 (Price et al., 2002). After choosing the visualisation parameter, all aggregated images will
231 be added to the map with default visualisation settings. Adjustments to visualisation
232 parameters can be made individually within the map's layer panel box (follow instructions
233 on Github link, see Data availability). All indices have a valid value range from -1 to 1 in
234 the web application. Google Earth Engine may encounter computational problems for
235 visualisation if the data is too large due to the size of the study area and/or the length of
236 the time period. This may lead to scaling error messages and some objects would not be
237 displayed on the map (or also *Console*). Visualisation problems, however, do not affect

238 image exports, which are always possible and only limited by the storage capacity of the
239 user's Google drive.

240 In addition to the visualisation options in Google Earth Engine, we provide an interactive
241 R Shiny application for visualising image time series (see Data availability).

242 Case examples

243 Example A shows deforestation in Brazil using historical Landsat images, while Example
244 B focusses on seasonal land cover changes in the city of Würzburg (Germany),
245 emphasising the enhanced level of detail provided by Sentinel-2 imagery. In both
246 examples a combination of three spectral bands (SWIR1-NIR-R; NIR-R-G) and a spectral
247 index (NDVI) are shown together with the number of valid pixels (see Fig. 1). The data
248 contain more spectral bands and indices not shown here.

249 In the Amazon rainforest, deforestation has become a pressing environmental concern
250 over the past several decades. Soy farms, along with other agricultural expansion, have
251 played a significant role in driving deforestation in the Amazon (Nepstad et al., 2006). We
252 used *GEE-PICX*, to generate and export annual image aggregates for an area in
253 Ariquemes, Rondônia, Brazil for 1991 and 2021, illustrating the magnitude of change over
254 three decades. Such annual aggregates (or composites) are suitable for inferences on
255 broad trends, but average seasonal dynamics or land cover changes within a year,
256 making them unsuitable e.g. for mapping floods.

257 The second example shows the seasonal changes in land cover/land use in the city centre
258 of Würzburg, Germany, and highlights the surrounding ring-shaped park. The region's
259 transition between summer and winter was captured in seasonal satellite image
260 composites and showcases the distinct phenological variations. The higher spatial
261 resolution of Sentinel-2 imagery allows better discrimination of small-scale features and
262 proves particularly valuable in the context of land cover and land use monitoring.
263 Seasonal variation in cloud cover can lead to seasonal bias in the available data. Snow
264 cover can also affect the quality of seasonal image compositions because the applied

265 cloud mask algorithm (see Supporting Information S2) does not perfectly mask highly
266 reflective surfaces such as clouds or snow in individual scenes.

267 Conclusion

268 Satellite imagery is essential for many environmental and conservation studies. However,
269 utilising freely available satellite products often requires expertise in data selection, pre-
270 processing, and substantial computational resources. Many environmental and
271 conservation studies therefore primarily rely on pre-packaged thematic products (Wong
272 et al., 2022), which may lack the detail necessary to address specific research questions.
273 *GEE-PICX* addresses these challenges by simplifying access to cloud-free satellite image
274 composites. It effectively addresses cloud cover issues, which are particularly problematic
275 in tropical or mountainous regions (Sanchez et al., 2020; Hribljan et al., 2017). Through
276 its intuitive interface, users can easily generate and export (multi-)temporal cloud-free
277 satellite images for any region, with data availability starting from 1984 (varying by
278 region).

279 *GEE-PICX* offers access to both Landsat and Sentinel-2 archives and provides
280 multispectral information complemented by various spectral indices and a data quality
281 metric. These are typically not or only partly present in the output of other platforms. *GEE-*
282 *PICX* is further set apart by its capability to process extensive areas with very large
283 download sizes. By making these rich satellite data archives accessible to non-remote-
284 sensing scientists and practitioners, *GEE-PICX* supports the integration of satellite data
285 into a wide range of environmental and conservation projects.

286 By lowering the barriers to satellite data analysis, *GEE-PICX* aims to bridge the gap
287 between satellite data availability and its practical use in environmental research and
288 conservation efforts.

289

290 Acknowledgements

291 We would like to express our gratitude to several individuals and organisations who have
292 played an important role in the successful completion of this project. First of all, we would
293 like to thank Marius Philipp, who gave us great technical support as a tutor during
294 workflow and app development in Google Earth Engine. Moreover, we thank Matthias
295 Baumann and Julian Oeser for insightful discussions about processing and utilisation of
296 satellite data time series. The work was financially supported by the Leibniz Institute for
297 Zoo and Wildlife Research and parts of the work were done during the implementation of
298 the USAID funded Biodiversity Conservation project in Viet Nam (7204402CA00001).

299 Conflict of Interest statement

300 The authors declare no conflicts of interest.

301 Author contributions

302 Jürgen Niedballa and Andreas Wilting conceived the idea, Luisa Pflumm led the
303 development of the GEE script and Hyeonmin Kang led the development of the GEE App
304 user interface. Luisa Pflumm developed the case examples. Luisa Pflumm, Jürgen
305 Niedballa and Andreas Wilting led the writing of the manuscript, and Hyeonmin Kang
306 contributed to the drafts. All authors gave final approval for publication.

307

308 Data availability

309 All necessary information for *GEE-PICX* is available in our GitHub repository:
310 <https://github.com/EcoDynIZW/GEE-PICX>. To use *GEE-PICX*, users need to log in to
311 Google Earth Engine with a Google account. The application opens in JavaScript code
312 editor mode (required for data export). Clicking the “Run” button opens the graphical user
313 interface. In the user interface, user inputs are specified and products can be exported to
314 users' Google drive. The repository includes a comprehensive step-by-step user guide.

315 Important note on no data values: When exporting rasters from GEE, all pixels with no
316 data are assigned a value of 0. This can affect subsequent analysis by misrepresenting
317 true no data values as 0. We provide an R script in the GitHub repository to convert these
318 misassigned 0 values back to no data. Users should apply this script to all GEE-exported
319 rasters before further analysis.

320 Additionally, we offer an R Shiny app on GitHub for visualising and querying time series
321 of annual images downloaded via *GEE-PICX*.

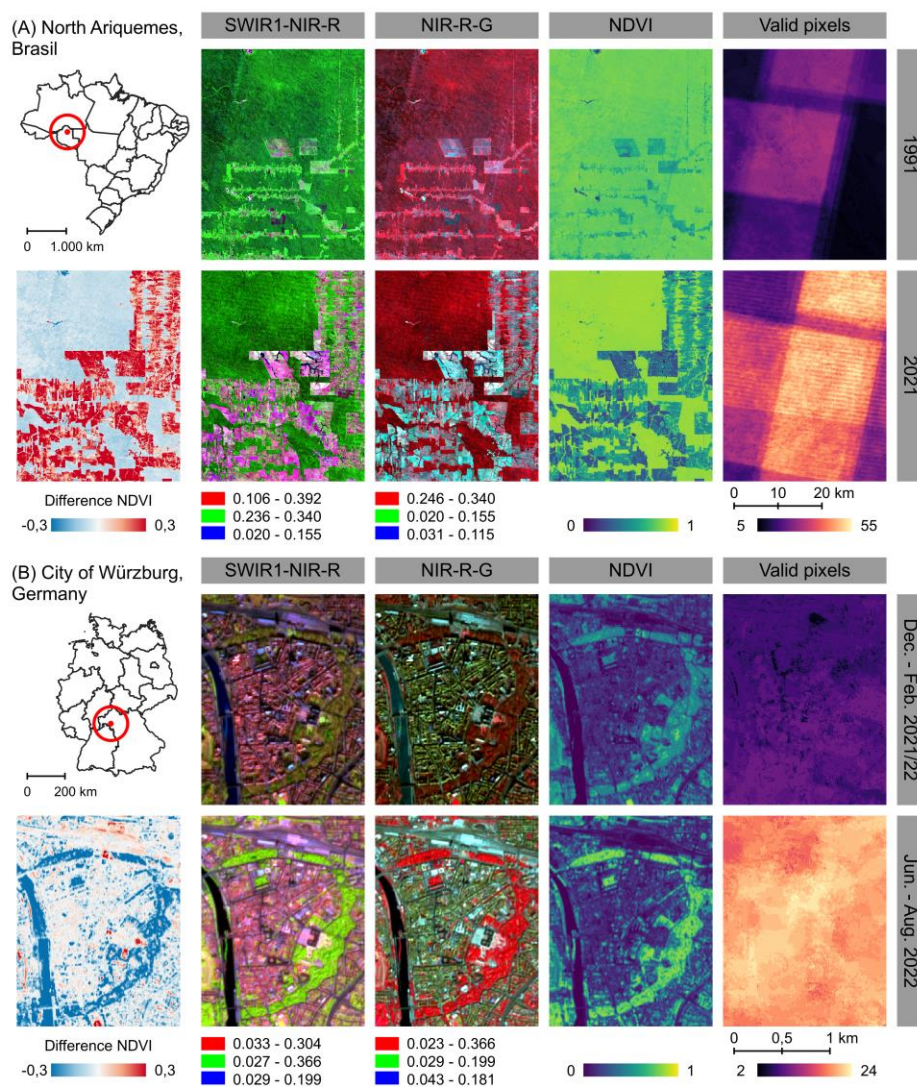
322

323 References

- 324 Aybar, C., Wu, Q., Bautista, L., Yali, R. and Barja, A., 2020. rgee: An R package for
325 interacting with Google Earth Engine. *Journal of Open Source Software*, 5(51), p.2272
- 326 Carrasco, L., O'Neil, A. W., Morton, R. D., & Rowland, C. S. (2019). Evaluating
327 combinations of temporally aggregated Sentinel-1, Sentinel-2 and Landsat 8 for land
328 cover mapping with Google Earth Engine. *Remote Sensing*, 11(3), 288.
- 329 Chaves, E.D.M., Picoli, C.A.M., & Sanches, D.I. (2020). Recent applications of Landsat
330 8/OLI and Sentinel-2/MSI for land use and land cover mapping: A systematic review.
331 *Remote Sensing*, 12(18), 3062.
- 332 Cord, A. F., Brauman, K. A., Chaplin-Kramer, R., Huth, A., Ziv, G., & Seppelt, R. (2017).
333 Priorities to advance monitoring of ecosystem services using earth observation. *Trends*
334 *in ecology & evolution*, 32(6), 416-428.
- 335 Google Earth Engine (2021). *Managing assets*. [https://developers.google.com/earth-](https://developers.google.com/earth-engine/guides/asset_manager)
336 [engine/guides/asset_manager](https://developers.google.com/earth-engine/guides/asset_manager) (accessed on 11 July 2023).
- 337 Guharajan, R., Mohamed, A., Wong, S. T., Niedballa, J., Petrus, A., Jubili, J., ... & Wilting,
338 A. (2021). Sustainable forest management is vital for the persistence of sun bear
339 Helarctos malayanus populations in Sabah, Malaysian Borneo. *Forest Ecology and*
340 *Management*, 493, 119270.
- 341 Guzman, R., Chepfer, H., Noel, V., Vaillant de Guélis, T., Kay, J. E., Raberanto, P., ... &
342 Winker, D. M. (2017). Direct atmosphere opacity observations from CALIPSO provide
343 new constraints on cloud-radiation interactions. *Journal of Geophysical Research:*
344 *Atmospheres*, 122(2), 1066-1085.
- 345 Hribljan, J. A., Suarez, E., Bourgeau- Chavez, L., Endres, S., Lilleskov, E. A.,
346 Chimbolema, S., ... & Chimner, R. A. (2017). Multidate, multisensor remote sensing
347 reveals high density of carbon- rich mountain peatlands in the páramo of Ecuador. *Global*
348 *change biology*, 23(12), 5412-5425.
- 349 Huntington, J.L., Hegewisch, K.C., Daudert, B., Morton, C.G., Abatzoglou, J.T., McEvoy,
350 D.J. and Erickson, T., 2017. Climate engine: Cloud computing and visualization of climate
351 and remote sensing data for advanced natural resource monitoring and process
352 understanding. *Bulletin of the American Meteorological Society*, 98(11), pp.2397-2410
- 353 Jiang, Z., Huete, A. R., Didan, K., & Miura, T. (2008). Development of a two-band
354 enhanced vegetation index without a blue band. *Remote sensing of Environment*,
355 112(10), 3833-3845.
- 356 Lasaponara, R., Abate, N., Fattore, C., Aromando, A., Cardettini, G., & Di Fonzo, M.
357 (2022). On the Use of Sentinel-2 NDVI Time Series and Google Earth Engine to Detect
358 Land-Use/Land-Cover Changes in Fire-Affected Areas. *Remote Sensing*, 14(19), 4723.

- 359 Mallinis, G., & Georgiadis, C. (2019). Editorial of Special Issue “Remote Sensing for Land
360 Cover/Land Use Mapping at Local and Regional Scales”. *Remote Sensing*, 11(19), 2202.
- 361 Montero, D., Aybar, C., Mahecha, M. D., Martinuzzi, F., Söchting, M., & Wieneke, S.
362 (2023). A standardized catalogue of spectral indices to advance the use of remote
363 sensing in Earth system research. *Scientific Data*, 10(1), 1-20.
- 364 Murray, N.J., Keith, D.A., Simpson, D., Wilshire, J.H. and Lucas, R.M., 2018. Remap: An
365 online remote sensing application for land cover classification and monitoring. *Methods*
366 *in Ecology and Evolution*, 9(9), pp.2019-2027
- 367 Nepstad, D. C., Stickler, C. M., & Almeida, O. T. (2006). Globalization of the Amazon soy
368 and beef industries: opportunities for conservation. *Conservation biology*, 20(6), 1595-
369 1603.
- 370 Parmes, E., Rauste, Y., Molinier, M., Andersson, K., & Seitsonen, L. (2017). Automatic
371 cloud and shadow detection in optical satellite imagery without using thermal bands—
372 Application to Suomi NPP VIIRS images over Fennoscandia. *Remote Sensing*, 9(8), 806.
- 373 Peter, B.G., Messina, J.P., Lin, Z. and Snapp, S.S., 2020. Crop climate suitability
374 mapping on the cloud: A geovisualization application for sustainable agriculture. *Scientific*
375 *Reports*, 10(1), p.15487.
- 376 Piao, S., Liu, Q., Chen, A., Janssens, I. A., Fu, Y., Dai, J., ... & Zhu, X. (2019). Plant
377 phenology and global climate change: Current progresses and challenges. *Global*
378 *Change Biology*, 25(6), 1922-1940.
- 379 Price, K. P., Guo, X., & Stiles, J. M. (2002). Optimal Landsat TM band combinations and
380 vegetation indices for discrimination of six grassland types in eastern Kansas.
381 *International Journal of Remote Sensing*, 23(23), 5031-5042.
- 382 Rudd, D. A., Karami, M., & Fensholt, R. (2021). Towards High-Resolution Land-Cover
383 Classification of Greenland: A Case Study Covering Kobbefjord, Disko and Zackenberg.
384 *Remote Sensing*, 13(18), 3559.
- 385 Sanchez, A. H., Picoli, M. C. A., Camara, G., Andrade, P. R., Chaves, M. E. D., Lechler,
386 S., ... & Queiroz, G. R. (2020). Comparison of Cloud cover detection algorithms on
387 sentinel-2 images of the amazon tropical forest. *Remote Sensing*, 12(8), 1284.
- 388 Storey, J., Scaramuzza, P., Schmidt, G., and Barsi, J. (2005). Landsat 7 scan line
389 corrector-off gap-filled product development. In *Proceedings of the Pecora 16 “Global*
390 *Priorities in Land Remote Sensing”* (Vol. 16, pp. 23–27). Sioux Falls, SD, USA.
- 391 Sinergise (2023a). *SentinelHub*. <https://www.sentinel-hub.com/> (accessed on 10 July
392 2023).

- 393 Sousa, D., & Small, C. (2023). Which vegetation index? Benchmarking multispectral
394 metrics to hyperspectral mixture models in diverse cropland. *Remote Sensing*, 15(4),
395 971.
- 396 United States Geological Survey (2022, August 4). *Landsat - Earth Observation Satellites*.
397 Fact Sheet 2015–3081, ver. 1.4, August 2022. Available at
398 <https://pubs.usgs.gov/fs/2015/3081/fs20153081.pdf>
- 399 United States Geological Survey (2023). *EarthExplorer*. <https://earthexplorer.usgs.gov/>
400 (accessed on 10 July 2023).
- 401 Verhoeven, V. B., & Dedoussi, I. C. (2022). Annual satellite-based NDVI-derived land
402 cover of Europe for 2001–2019. *Journal of Environmental management*, 302, 113917.
- 403 Weng, Q., Quattrochi, D., Xian, D. (2008). *Special Issue Remote Sensing of Land Surface*
404 *Properties, Patterns and Processes*. MDPI Remote Sensing. Available at
405 [https://www.mdpi.com/journal/sensors/special_issues/remote-sensing-land-surface-](https://www.mdpi.com/journal/sensors/special_issues/remote-sensing-land-surface-properties#published)
406 [properties#published](https://www.mdpi.com/journal/sensors/special_issues/remote-sensing-land-surface-properties#published) (accessed on 11 July 2023).
- 407 Wong, S. T., Guharajan, R., Petrus, A., Jubili, J., Lietz, R., Abrams, J. F., ... & Sollmann,
408 R. (2022). How do terrestrial wildlife communities respond to small- scale Acacia
409 plantations embedded in harvested tropical forest?. *Ecology and Evolution*, 12(9), e9337.
- 410 Wu, Q., 2020. geemap: A Python package for interactive mapping with Google Earth
411 Engine. *Journal of Open Source Software*, 5(51), p.2305
- 412 Yang, W., Chen, X., Wang, C., Cao, R., Zhu, X., Shen, B. (2021). *Special Issue Time*
413 *Series Analysis in Remote Sensing: Algorithm Development and Applications*. MDPI
414 Remote Sensing.
415 [https://www.mdpi.com/journal/remotesensing/special_issues/time_series_algorithm_dev](https://www.mdpi.com/journal/remotesensing/special_issues/time_series_algorithm_development)
416 [elopment](https://www.mdpi.com/journal/remotesensing/special_issues/time_series_algorithm_development) (accessed on 11 July 2023).
- 417 Yin, H., Brandão Jr, A., Buchner, J., Helmers, D., Iuliano, B. G., Kimambo, N. E., ... &
418 Radeloff, V. C. (2020). Monitoring cropland abandonment with Landsat time series.
419 *Remote Sensing of Environment*, 246, 111873.
- 420 Zeng, Y., Hao, D., Huete, A., Dechant, B., Berry, J., Chen, J. M., ... & Chen, M. (2022).
421 Optical vegetation indices for monitoring terrestrial ecosystems globally. *Nature Reviews*
422 *Earth & Environment*, 3(7), 477-493.
- 423 Zhu, C., Zhang, X., & Huang, Q. (2018). Four decades of estuarine wetland changes in
424 the Yellow River delta based on Landsat observations between 1973 and 2013. *Water*,
425 10(7), 933.
- 426 Zhu, Z., Wang, S., & Woodcock, C. E. (2015). Improvement and expansion of the Fmask
427 algorithm: Cloud, cloud shadow, and snow detection for Landsats 4–7, 8, and Sentinel 2
428 images. *Remote sensing of Environment*, 159, 269-277.

429 **Figures**

Options	(A) North Ariquemes (Brasil)	(B) City of Würzburg (Germany)
Satellite platform	Landsat-5,7,8,9	Sentinel-2
Study area	Polygon coordinates (in degree): -63.1 to -62.6 °W, -9.7 to -9.3 °S	Polygon coordinates (in degree): 49.78 to 49.8 °E, 9.92 to 9.94 °N
Month, year, max. cloud cover (per scene)	(1) 1-12, 1991, 65% (2) 1-12, 2021, 65%	(1) 12-2, 2022-23, 65% (winter) (2) 6-8, 2022, 65% (summer)
Number of selected scenes	(1) 44 scenes (2) 97 scenes	(1) 9 scenes (2) 26 scenes
Band selection	B, G, R, NIR, SWIR1, SWIR2, NDVI, valid pixels	
Aggregation mode	median	
Spatial resolution	30 meter	10 meter
CRS	UTM (EPSG: 32620)	UTM (EPSG: 32632)

430
431 **Figure 1:** Example GEE-PICX products. A: Annual aggregates based on Landsat scenes for
432 1991 and 2021. B: Seasonal aggregates based on Sentinel-2 scenes for summer (June 2022 -
433 August 2022) and winter (December 2021 - February 2022). The maps show a subset of the
434 available band information. The striking pattern in the valid-pixel scenes results from the orbital
435 path overlap of the Landsat satellites and does not affect image composites.

Supporting Information

Supporting Information S1

Table S1: Comparison of available tools and applications which allow for satellite image processing similar to GEE-PICX.

	Geospatial platforms				Packages			Analysis tools	
Tool name	GEE-PICX	Climate Engine	Sentinel Hub	Earth Explorer	Awesome Spectral Indices	geemap	rgee	REMAP	CropSuit GEE
Website	https://github.com/EcoDynI/ZW/GEE-PICX	https://app.climateengine.org/climateEngine	https://apps.sentinel-hub.com/eo-browser/	https://earthexplorer.usgs.gov/	https://github.com/awesome-spectral-indices/awesome-spectral-indices	https://github.com/gee-community/geemap	https://github.com/r-spatial/rgee	https://remap-app.org/remap	https://dataverse.harvard.edu/dataset.xhtml?persistentId=doi:10.7910/DVN/UFC6B5
Purpose	Data acquisition, visualisation, export	Data acquisition, visualisation, export	Data acquisition, visualisation, export	Data acquisition, visualisation, export	Spectral Indices Catalog	GEE access for python users	GEE access for R users	Land-cover/Land-use classification	Crop-Climate-Suitability Mapping
Graphical user interface	Yes	Yes	Yes	Yes	No	No	No	Yes	No
Coding required	Optional ¹	No	Optional	No	Yes	Yes	Yes	No	Optional
Language	GEE Javascript API	-	Sentinel Hub API	-	GEE Javascript API, Python, Julia, R	Python	R	-	GEE Javascript API

Data sources	Sentinel-2, Landsat	> 10 different datasets ²	> 10 different datasets ²	> 10 different datasets ²	Entire GEE catalogue	Entire GEE catalogue	Entire GEE catalogue	Landsat & climate data	MODIS & climate data
Time Range	1984 - present; custom month range	1984 - present; custom date range	1972 - present; custom date range	1972 - present; custom date range	Custom	Custom	Custom	No	2000 - 2017; custom date range
Cloudfree mosaics	Yes	Yes	Yes	No	User-specific	User-specific	User-specific	No	No
Custom cloud cover value	Yes	No	No	Yes	User-specific	User-specific	User-specific	No	No
Spectral indices calculation	Yes	Yes	Yes	No	Yes	User-specific	User-specific	Yes	No
Data quality assessment	Yes ³	Yes ⁴	No	No	User-specific	User-specific	User-specific	No	No
Data visualisation	Yes	Yes	Yes	Yes	User-specific	User-specific	User-specific	Yes	Yes
Export product	Aggregated multi-band mosaic(s)	Aggregated single-band mosaic(s)	Aggregated multi-band mosaic(s)	Single product(s)	User-specific	User-specific	User-specific	Classification map	
Export limitation	Unlimited ⁵	10,000 x 10,000 pixel	2,500 x 2,500 pixel	10,000 products	Unlimited	Unlimited	Unlimited	100,000 km ²	Unlimited ⁵
Reference	Pflumm et al., 2024	Huntington et al., 2017	Sinergise, 2023a	United States Geological Survey, 2023	Montero et al., 2023	Wu, 2020	Aybar et al., 2020	Murray et al., 2018	Peter et al., 2020

¹ Only for adding custom spectral indices to app

² Several datasets from satellite, climate, hazard, forecast (see websites for list of data)

³ Add valid-pixel band

⁴ Calculate statistics

⁵ maxPixels of 10,000 can be exceeded, only limited by Earth Engine Quota (<https://developers.google.com/earth-engine/guides/usage>) and Google Drive storage capacity

Supporting Information S2

Data processing in GEE-PICX

Table S2: Functional setup of GEE-PICX application script.

Functionality	Description
Image selection and filtering	Select Landsat / Sentinel-2 surface reflectance (SR) products (Level-2). Filter single scenes by study area, time frame and maximum cloud cover.
Cloud masking *	Landsat SR data: mask clouds, cloud shadows and snow from the Cloud Quality Assessment band (QA_PIXEL bitmask). Sentinel-2 SR data: mask clouds, cloud shadows and highly reflective surfaces with auxiliary S2 cloud probability data set (s2cloudless).
Band selection	Select and rename S2 bands according to spectral wavelength range Select and rename LS 8 & 9 bands according to spectral wavelength range Select and rename LS 5 & 7 bands according to spectral wavelength range
Scale factor application	Apply scale factor for Landsat SR data (0.0000275) and add offset value (- 0.2) before usage Apply scale factor for Sentinel-2 SR data (0.0001)
Spectral indices calculation	Calculate indices with respective formulas and add as band information to each individual scene
Image aggregation & data quality assessment	Aggregate filtered scenes from year or season by median, mean or standard deviation Count valid pixels at each pixel location for data quality assessment
Visualisation	Aggregated scenes can be added to the map. Users can choose spectral indices as single bands or choose from various 3-band combinations. Further changes can be applied manually in the layer panel box. May fail if data size or area of interest are too large (limitations in Google Earth Engine).
Export preparation	Create a batch task to export images as raster to Google Drive. All image band values are multiplied by 10,000 in advance and converted to signed 16-bit integer to reduce output file size (except for valid-pixel band)

* Additional information on s2cloudless:

The development of the s2cloudless algorithm (Zupanc, 2019), however, has allowed researchers to refine cloud masking, resulting in greater confidence in the final analysis. There is currently no equivalent method for images from the Landsat collection. While the QA60 band is limited to a binary classification of thick and cirrus clouds (European Space Agency, 2020), s2cloudless generates an image with cloud presence

probabilities ranging from 0 to 100 percent, at 10 metre scale (Braaten et al., 2020). This provides the opportunity to customise the cloud masking process to better suit the specific requirements of a project. Higher values of the s2cloudless layer are more likely related to clouds or highly reflective surfaces such as snow or roof tops (Google Earth Engine, 2023).

The s2cloudless layer is a separate data set from which matching scenes are automatically selected and filtered. The default cloud probability threshold in the application is 50 % to define cloud / non-cloud masks, which generally allows a very good cloud masking performance (Braaten et al., 2020). The optimal value for the best performance can depend on factors such as cloud type, cover type, location, etc. Users who wish to further customise the cloud mask need to adjust the variable “isNotCloud” in the application script where cloud masking is applied to the selected Sentinel-2 images. In this case, we suggest experimenting with a few different values to better understand the distribution of cloud probability values. For example, thin clouds may not be detected at 90 % cloud probability threshold, but are detected at 10 % (Braaten et al., 2020). The single scenes from the cloud-masked image collection in the *Console* tab could be used to investigate changes due to cloud mask tuning. Nevertheless, for proper inspection and evaluation, basic knowledge of using the Google Earth Engine API is beneficial. For most use cases it is not necessary to modify the cloud probability threshold.

References

Braaten, J., Schwehr, K., Ilyushchenko, S. (2020). *More accurate and flexible cloud masking for Sentinel-2 images*. Available online: <https://medium.com/google-earth/more-accurate-and-flexible-cloud-masking-for-sentinel-2-images-766897a9ba5f> (accessed on 11 July 2023).

European Space Agency (2022). *Sentinel-2*. ESA. Sentinel-2 User Handbook; ESA: Paris, France, 2015; p. 64. Available at: https://sentinel.esa.int/documents/247904/685211/Sentinel-2_User_Handbook.

Google Earth Engine (2023). *Sentinel-2: Cloud Probability*. Available online: https://developers.google.com/earth-engine/datasets/catalog/COPERNICUS_S2_CLOUD_PROBABILITY#description (accessed 11 July 2023).

Zupanc, A (2019). *Improving Cloud Detection with Machine Learning*. Available online: <https://medium.com/sentinel-hub/improving-cloud-detection-with-machine-learning-c09dc5d7cf13> (accessed on 11 July 2023).

Supporting Information S3

Satellite data available in GEE-PICX

Table S3: Information on satellite data accessible from GEE-PICX web application.

Platform	Sentinel-2		Landsat			
Mission	Sentinel-2A	Sentinel-2B	Landsat-5	Landsat-7	Landsat-8	Landsat 9
Mission Launch	2015-06-23	2017-03-07	1984-03-01	1999-04-15	2013-02-11	2021-09-27
Data availability in GEE-PICX app	2017-03-28 - present		1984-03-16 - 2012-05-05	1999-05-28 - present	2013-03-18 - present	2021-10-31 - present
Sensor*	MSI		MSS + TM	ETM+	OLI + TIRS	OLI + TIRS
Temporal resolution	10-days each, 5-days combined constellation			16-days each, 8-days combined constellation Landsat-8 and 9		
Spatial resolution	10-metre			30-metre		
Spectral resolution**	<i>Bands 2-5, 8, 8A, 11-12:</i> visible, NIR, red-edge, SWIR		<i>Bands 1-5, 7</i> visible, NIR, SWIR		<i>Bands 2-7</i>	
Spectral & spatial resolution (bands, in meter)	<i>Bands 2-5, 8, 8A, 11-12:</i> 10 m: R, G, B, NIR; 20 m: Red-edge, SWIR		<i>Bands 1-5, 7:</i> 30 m: B, G, R, NIR, SWIR	<i>Bands 1-5, 7:</i> 30 m: B, G, R, NIR, SWIR	<i>Bands 2-7:</i> 30 m: B, G, R, NIR, SWIR	<i>Bands 2-7:</i> 30 m: B, G, R, NIR, SWIR
Additional information	-	-	-	Scan Line Corrector (SLC) failure since 2003-05-31 (22 percent of each image affected by data gaps)	-	-
Operator***	ESA			NASA & USGS		

* OLI, Operational Land Imager; TIRS, Thermal Infrared Sensor; ETM+, Enhanced Thematic Mapper Plus; TM, Thematic Mapper; MSS, Multispectral Scanner; MSI, Multispectral Instrument

** Visible: blue, green, red; NIR: near-infrared; SWIR: shortwave-infrared

*** ESA, European Space Agency; NASA, National Aeronautics and Space Administration; USGS, United States Geological Survey

Supporting Information S4

Spectral Indices available in GEE-PICX

Table S4: Available spectral indices derived from Landsat or Sentinel-2 imagery.

Band name	Full name	Formula	Group	Interpretation
NDVI	Normalised Difference Vegetation Index	$\frac{(NIR - Red)}{(NIR + Red)}$	Vegetation Index	Highlights density and health of photosynthetically active vegetation. Tends to saturate in densely vegetated areas. Sensitive to the contribution of soil brightness and atmospheric effects.
EVI	Enhanced Vegetation Index	$2.5 * \frac{(NIR - Red)}{(NIR + 6 * Red - 7.5 * Blue + 1)}$	Vegetation Index	Highlights photosynthetically active vegetation, but does not saturate in densely vegetated areas. Accounts for soil brightness variation. Less affected by atmospheric effects than NDVI.
SAVI	Soil-Adjusted Vegetation Index	$\frac{(NIR - Red)}{(NIR + Red + L)} * (1 + L)$	Vegetation Index	Highlights photosynthetically active vegetation and accounts for soil brightness variation.
MSAVI	Modified Soil-Adjusted Vegetation Index	$\frac{(NIR - Red)}{(NIR + Red + L_0)} * (1 + L_0)$	Vegetation Index	Modified version of SAVI to further minimise the soil background influences on the vegetation signal.
GNDVI	Green Normalised Difference Vegetation Index	$\frac{(NIR - Green)}{(NIR + Green)}$	Vegetation Index	Highlights the density and health of photosynthetically active vegetation. It is sensitive to chlorophyll content, making it effective for assessing green crop biomass. May saturate in dense vegetation but is generally less influenced by soil brightness and atmospheric effects compared to NDVI.
NDMI	Normalised Difference Moisture Index	$\frac{(NIR - SWIR1)}{(NIR + SWIR1)}$	Water & Moisture Index	Sensitive to moisture levels in vegetation and soil. Useful for vegetation analyses, for identifying areas prone to drought stress or excess moisture.
NDWI	Normalised Difference Water Index	$\frac{(Green - NIR)}{(Green + NIR)}$	Water & Moisture Index	Sensitive to water bodies. Useful for water resource management, wetland monitoring, and flood assessment.

NBR	Normalised Burn Ratio	$\frac{(NIR - SWIR2)}{(NIR + SWIR2)}$	Burn & Fire Index	Detects and quantifies burnt areas. In general, low NBR values indicate recently burnt areas and bare ground.
BSI	Bare Soil Index	$\frac{(SWIR1 + Red) - (NIR + Blue)}{(SWIR1 + Red) + (NIR + Blue)}$	Built-up & Urban Index	Highlights bare ground and rock surfaces. Useful in identification of soil erosion, land degradation, and urbanisation processes.
NDBI	Normalised Difference Built-up Index	$\frac{(SWIR1 - NIR)}{(SWIR1 + NIR)}$	Built-up & Urban Index	Highlights built-up and urban areas by contrasting impervious surfaces with vegetation. Higher NDBI values indicate the presence of buildings and other man-made structures.
NDSI	Normalised Difference Snow Index	$\frac{(Green - SWIR1)}{(Green + SWIR1)}$	Snow & Ice Index	Detects snow cover by differentiating snow from clouds and other land surfaces. High NDSI values indicate snow-covered areas, making it useful for monitoring snow extent and water resource management.

For more information on spectral indices see: Petropoulos & Kalaitzidis (2012), Zeng et al. (2022), United States Geological Survey (2022), Qi et al. (1994), Keeley (2009).

References

- Gibson, R. K., White, L. A., Hislop, S., Nolan, R. H., & Dorrrough, J. (2022). The post-fire stability index; a new approach to monitoring post-fire recovery by satellite imagery. *Remote Sensing of Environment*, 280, 113151.
- Jiang, Z., Huete, A. R., Didan, K., & Miura, T. (2008). Development of a two-band enhanced vegetation index without a blue band. *Remote sensing of Environment*, 112(10), 3833-3845.
- Keeley, J. E. (2009). Fire intensity, fire severity and burn severity: a brief review and suggested usage. *International journal of wildland fire*, 18(1), 116-126.
- Key, C. H., & Benson, N. C. (2006). Landscape assessment (LA). *FIREMON: Fire effects monitoring and inventory system*, 164, LA-1.
- Petropoulos, G. P., & Kalaitzidis, C. (2012). Multispectral vegetation indices in remote sensing: an overview. *Ecological Modeling*, 2, 15-39.

Qi, J., Chehbouni, A., Huete, A. R., Kerr, Y. H., & Sorooshian, S. (1994). A modified soil adjusted vegetation index. *Remote sensing of environment*, 48(2), 119-126.

Shanahan, J. F., Schepers, J. S., Francis, D. D., Varvel, G. E., Wilhelm, W. W., Tringe, J. M., ... & Major, D. J. (2001). Use of remote-sensing imagery to estimate corn grain yield. *Agronomy journal*, 93(3), 583-589.

Sousa, D., & Small, C. (2023). Which vegetation index? Benchmarking multispectral metrics to hyperspectral mixture models in diverse cropland. *Remote Sensing*, 15(4), 971.

United States Geological Survey (2022, August 4). *Landsat - Earth Observation Satellites*. Fact Sheet 2015–3081, ver. 1.4, August 2022. Available at <https://pubs.usgs.gov/fs/2015/3081/fs20153081.pdf>

Zeng, Y., Hao, D., Huete, A., Dechant, B., Berry, J., Chen, J. M., ... & Chen, M. (2022). Optical vegetation indices for monitoring terrestrial ecosystems globally. *Nature Reviews Earth & Environment*, 3(7), 477-493.